

**Semi-empirical model
for prediction of the
Top-Of-the-Line corrosion risk**

**Frederic Vitse
NSF I/UCRC, Corrosion in Multiphase Systems Center
Institute for Corrosion and Multiphase Technology
Ohio University, Athens, OH 45701, U.S.A**

**Dr. Khairul Alam
Mechanical Engineering Department
Ohio University, Athens OH 45701.**

**Yves Gunaltun, Dominique Larrey de Torreben, Pierre Duchet-Suchaux
Exploration and Production TotalFinaElf
92069 Paris La Defense.**

ABSTRACT

A model is proposed that determines the influence of the condensation rate on the Top-of-Line Corrosion (TLC) under dewing conditions. The model is based on an analytical and numerical solution of the flow field in the falling film of the condensate. A numerical solution is then used to compute the mass transfer by convection and diffusion of the dissolved species. At the wall, the boundary conditions are given by empirical equations for the corrosion rate. The numerical solutions are compared with data from the field observations.

INTRODUCTION

For economical reasons, multiphase wet gas is being sent unprocessed into pipelines rather than being dried prior to transportation. Obviously, dry gas transportation has strong advantages; problems linked with the presence of water in the line such as liquid holdup, slugging, hydrates formation and corrosion can be avoided. But, considering the high cost of offshore processing, wet gas transportation is now common practice. Thus, intensive research has been carried by the oil & gas companies to understand the problems related to transport of unprocessed fluids.

Top of the line corrosion (TLC) is one of the forms of corrosion specific to wet gas transportation with stratified flow pattern. It occurs mainly when significant heat transfer is possible between the warm unprocessed produced fluids and a cold surrounding such as deep-sea water, river water, or frozen land. Under large temperature gradients, the water contained in the gas phase will condense on the pipe wall. Obviously, the higher the water vapor content the larger the condensation rate. Under gravity forces, the condensed water drains to the bottom where it accumulates. Thus, the corrosion can be expected to occur at the bottom of the pipe where all the condensed water and produced liquids collect. However, under sustained dewing conditions, a thin film of condensed water will form around the pipe in contact with the gas phase, allowing carbon dioxide, organic acids, or hydrogen sulfide to dissolve. In the presence of such corrosive agents, corrosion occurs at the top of the line as well.

LITERATURE REVIEW

The TLC phenomenon was observed as early as 1960, when a case of TLC was reported in the sour gas field of Lacq in France. Some of the parameters leading to TLC were reported by Estavoyer⁽¹⁾ in 1981. The author observed that low gas velocities leading to stratified or stratified-wavy flow regime are necessary for TLC to take place. Under such flow regimes, the inhibitors injected to minimize the corrosion occurring at the bottom of the line could not reach the corrosion-exposed area at the top. This observation was confirmed by the fact that no corrosion was detected at the top of a line with an annular inhibited flow.

In the last decade, TLC has been subject to increasing research in view of the multiplication of the pipeline failures due to such corrosion. In 1991, Olsen and Dugstad⁽²⁾ made a systematic research on the parameters influencing TLC. Of primary interest was the influence of temperature on the products of corrosion, namely iron carbonate. It appears that at high temperature (70°C and above) and low condensation rate, a protective film of iron carbonate forms at the surface of the wall. This film still exists, but is no longer protective when the temperature drops (50°C and below) and can be wiped off easily. The authors interpreted the results on the formation of a film by concluding that the condensation rate in this case is not high enough to lower the iron ions concentration below the saturation point for iron carbonate to precipitate. It appears therefore that there exists a critical condensation rate above which saturation of the condensed water is not longer saturated by the products of corrosion. In the case of TLC where the continuous injection of inhibitors doesn't minimize the corrosion rate, the formation of a natural protective layer is a fundamental way of controlling corrosion. Thus, a perfect understanding on how and when this protective layer forms is a key point of TLC remediation. Olsen and Dugstad also studied the influence of the gas flowrate on the corrosion rate. The higher the gas flow rate, the higher is the observed corrosion rate. An increase in gas flow rate would also correspond to an increase in condensation rate. According to this, it can be concluded that the gas flow rate influences the condensation rate, which in turn influences the corrosion rate. The authors concluded that four cases are possible:

- At very high condensation rates, the steel is washed with almost pure CO₂-water mixture (the concentration of products of corrosion is negligible and doesn't influence the corrosion rate) and the corrosion rate can reach several mm/yr. No iron carbonate was observed on the steel surface.
- At high condensation rates (above the critical condensation rate), corrosion is reduced due to accumulation of corrosion products (even if saturation is not reached). The corrosion rate is

governed by the rate of the corrosion reaction and the rate of condensation, which increases and decreases the iron concentration, respectively. The iron concentration at which these two counteracting reactions are balanced determines the corrosion rate.

- At low condensation rate (below the critical condensation rate) and low temperature, a non-protective scale will form. The iron ion concentration remains constant, as does the pH of the solution. The condensation rate doesn't influence the corrosion rate anymore. A balance is achieved between the film build up and the film removal and the maximum corrosion rate is that corresponding to saturated water.
- At lower condensation rates (below the critical condensation rate) and high temperature, a protective film forms. The solubility product of iron carbonate in water is lowered, thus reducing the saturation level in the water. As a consequence, the maximum corrosion rate is decreased.

Olsen and Dugstad did not develop any mechanistic model or correlation to relate the corrosion rate with temperature, condensation rate, gas flowrate, or iron concentration. One can already realize the complex influence of temperature: higher gas temperature tend enhance the corrosion rate by increasing the condensation rate but also minimize the corrosion if the saturation conditions are reached and a protective scale is formed.

In 1993, de Waard⁽³⁾ developed an empirical model allowing calculation of the corrosion rate in full pipe flow as a function of the temperature, partial pressure of CO₂, and pH of the solution. This model predicts the corrosion rate with a respectable degree of accuracy for full pipe flow but would give very conservative results if applied to the TLC. In order to adapt his model to the dewing conditions, de Waard introduced a correcting factor $F=0.1$ for the TLC case assuming any condensation rate below an experimental critical condensation rate of 0.25 ml/m²/s. The simplicity of this model makes it easy to apply. However, the values predicted do not always fit the experimental ones⁽⁵⁾.

It is not before 1999 and the case history presented by Gunaltun⁽⁴⁾ that a complete description of a TLC case was fully made. Gunaltun reported the visual inspection of a wet gas pipeline from the field that suffered severe TLC damages. This description provides a better understanding of the TLC process. First, it comes out from the visual observation that three areas of the pipe wall must be considered independently because they are subject to different corrosive conditions:

- The bottom of the line is subject to uniform corrosion at a low rate due to injected inhibitors.
- The top of the line (from 10 o'clock to 2 o'clock) is covered with a partially protective carbonate scale and with several deep pits.
- The sidewall is uniformly corroded at a much higher rate than the bottom. No carbonate scale formed on this surface. This was explained by the author to be the consequence of a "washing effect": as the water condenses, it drains to the bottom of the pipe under its gravity. Whereas at the top of the line, the surface tension of water leads to the formation of droplets saturated by corrosion products, thus allowing the partial formation of a carbonate scale.

The corrosion rates measured were an order of magnitude larger than the one obtained experimentally by Olsen and Dugstad (as high as 2 mm/y) for a condensation rate of approximately 1.5 ml/m²/s. The reason for the observed difference could be due to the presence of pitting corrosion. Gunaltun concluded that the influence of the condensation rate, and particularly the value of the critical condensation rate are extremely important in TLC.

In 2000, Pots⁽⁵⁾ published a paper focusing on the TLC under scaling conditions. The author used the “iron supersaturation model”⁽⁶⁾ to describe the evolution of the corrosion rate as a function of the iron discharge via the condensation rate and as a function of the precipitation rate for the carbonate scale. By comparing with other models and experimental data^{(2),(4)}, Pots confirmed that de Waard’s model is too conservative and the saturation model introduced by Oddo and Tomson⁽⁷⁾ is too optimistic. Thus, the supersaturation model can be considered to be the most accurate model available for TLC under scaling conditions. This model confirms that the role played by the condensation rate is very important in determination of TLC. In his analysis, Pots proposed a model for computation of a condensation rate in horizontal pipelines in presence of non-condensable gases by considering the mass transfer across the gas boundary layer to be the limiting factor. Also the author suggests using a heat transfer model to calculate the inner wall temperature, which is needed for the computation of the precipitation rate.

Following the case history published one year before, Gunaltun and Larrey⁽⁸⁾ correlated the corrosion rate with the calculated condensation rates for the specific pipeline of the Tunu field⁽⁴⁾. The computation was done by the use of thermodynamics, hydrodynamics, and thermal exchanges packages. This complete approach shows the complexity of determining the actual condensation rate inside a pipeline. The first step is to determine the composition of each phase by assuming that the different phases are at steady state. The equation of state chosen in this case is the Soave-Redlich-Kwong equation. Secondly, a hydrodynamic package is needed to determine the actual flow regime and confirm that the TLC can occur at a specific location in the pipeline. By coupling this hydrodynamic package (Tacite) to a thermal exchange package, it is possible to calculate the local temperature and axial velocity of each phase at a given point of the line. The thermal exchange package determines the radial heat transfer in the pipeline for a steady state flow. The associated thermal resistance has 3 components:

- The external resistance is due to the surrounding medium (external wall to bulk of the surrounding fluid).
- The diffusion resistance (conduction) in the pipe wall, coating and insulation layers.
- The inner resistance is due to the convective flow in the pipe (inner wall to gas bulk).

Considering the actual body of knowledge on how to calculate the inner resistance, the authors adapted a global thermal resistance to fit the data on the temperature profile collected in their pipeline. There is a real need of calculating the inner thermal resistance if one wants to obtain an accurate value of the heat transferred during TLC and thus an accurate condensation rate. According to the visual inspection and the calculated condensation rates, Gunaltun and Larrey concluded from this study that the critical condensation rates is $0.25 \text{ ml/m}^2/\text{s}$ if the considered condensation surface is the top half of the inner pipe or $0.15 \text{ ml/m}^2/\text{s}$ if the gas-wetted surface under stratified flow regime is considered. They also confirmed that the influence of the gas flow rate is significant as well as the influence of the inlet temperature of the effluents. Gunaltun emphasized the importance of studying the critical condensation rate to properly determine the TLC rate. The author also introduces the idea that the critical water condensation rate is not unique but rather a function of temperature and the organic acid content of the production water.

Another paper on TLC published in 2000 was presented by Edwards⁽⁹⁾ and focused one more time on the influence of different parameters on the TLC during flow in pipelines. In agreement with Gunaltun⁽⁴⁾, Edwards confirmed that no inhibition of the top of the line was possible under stratified flow regime. When corrosion takes place, he also observed that the products of corrosion, namely the

bicarbonate ions, would buffer the pH of the solution thus diminishing the corrosion rate from its value under pure water condensation. It is interesting to note that Edwards suggested a way to calculate the corrosion rate when no saturation of the condensed water is possible. At high condensation rate, a continuous sheet of water should form and Edwards suggests using the de Waard model⁽³⁾ for the computation of the corrosion rate. Since the water is refreshed very quickly, the author also suggests taking the pH of condensed water at a low level, namely 3.6. In the case of a gradual cooling of the gas, Edwards mentioned that the occurrence of corrosion should follow a statistical function according to where a water droplet would happen to form. The author concluded that if a sufficient understanding of the conditions present in the pipeline is achieved, the prediction of the location and severity of water drop is possible. Hence, an estimation of the TLC could be achieved. However, the author mentions the difficult task of achieving such a prediction of the TLC according to the fact that multiple type of corrosion occur during TLC.

Recently, some more papers have been published by Schmitt⁽¹⁰⁾ and Gunaltun⁽¹¹⁾ on how to control the TLC by the use of spreading agents for inhibitors and inhibitors batch treatment respectively and how to neutralize organic acids. These two papers show that currently the answer for TLC prevention is not known or that it can't be achieved without high expense in batch treating.

This paper presents a method on how to calculate the condensation rate that occurs in wet gas conditions when the only components present are water and carbon dioxide. The profile of the thin film that condenses on the inner pipe wall is determined according to the condensation rate calculated in this model. Then, the momentum, energy and mass transfer equations are solved within the film and an empirical model⁽³⁾ for corrosion rate is taken as a boundary condition at the wall.

PRESENTATION OF THE MODEL

The falling film theory

As it was previously mentioned, the water condensing on the wall forms a thin film where carbon dioxide dissolves. The film profile was obtained by adapting Nusselt's theory of filmwise condensation⁽¹²⁾ to the case of an horizontal pipe. Using this theory, the local film thickness and the local heat transfer coefficient across the liquid film where determined:

$$\delta(\varphi) = \left[\frac{4 \times A \times R \times \lambda_1 \times (T_{sat} - T_{wall}) \times \int (\sin \varphi)^{1/3} d\varphi}{(\sin \varphi)^{4/3}} \right]^{1/4} \left[\left(B + \frac{15 \times C'}{24} \right) \times \rho_l \times (\rho_l - \rho_g) \times g \times \Delta h_v(T_{sat}) \right]^{-1/4} \quad (1)$$

$$h_1(\varphi) = \left[\frac{\left(B + \frac{15 \times C'}{24} \right) \times \lambda_1^3 \times \rho_1 \times (\rho_1 - \rho_g) \times g \times \Delta h_v(T_{\text{sat}})}{4 \times A \times R \times (T_{\text{sat}} - T_{\text{wall}}) \times \frac{\int (\sin \varphi)^{1/3} d\varphi}{(\sin \varphi)^{4/3}}} \right]^{1/4} \quad (2)$$

The symbol φ represents the circumferential angle in the cross section of the pipe as shown in Figure 1. The velocity profile in the liquid film leading to the previous equations is parabolic and the temperature profile in the same liquid film is assumed linear according to Nusselt's theory⁽¹²⁾. Equation 2 solved together with the equation of the energy balance at the wall (see Figure 2) gives the temperature at the wall. The energy balance at the wall is given by:

$$\dot{q}(\varphi) = \frac{\lambda_{\text{wall}}}{l} \times (T_{\text{wall}} - T_{\text{ext}}) = \frac{\lambda_1}{\delta} \times (T_{\text{sat}} - T_{\text{wall}}) \quad (3)$$

Knowing the wall temperature, the heat flux through the wall can be calculated and the condensation rate is obtained by writing:

$$\dot{m}(\varphi) = \frac{\dot{q}}{\Delta h_{\text{vap}}(T_{\text{sat}})} \quad (4)$$

Once the profile of the film thickness is computed, one can solve the mass transfer equations for corrosive species and products of corrosion within the condensate film. This is achieved by considering that the transport of species occurs by diffusion and convection in the radial direction and by convection only in the orthoradial direction. The method used was the finite-difference method with an upwind scheme in both directions. At the gas-liquid interface, the boundary condition was derived from Henry's law (for the computation of the surface concentration of dissolved carbon dioxide) and the temperature was taken equal to the saturation temperature of the water vapor in a carbon dioxide-water vapor mixture. In order to calculate such a saturation temperature, the assumption of ideal gas mixture was made and Antoine's law was used:

$$y_w \times P = x_w \times P_w^{\text{sat}} \quad (\text{ideal gas law or Raoult's law}) \quad (5)$$

$$\log(P_w^{\text{sat}}) = A' - \frac{B'}{T_{\text{sat}} + C'} \quad (\text{Antoine's law}) \quad (6)$$

The values obtained were compared with the experimental data published by Fenghour⁽¹³⁾. Results are shown in Figure 3. In general, a good agreement is obtained for a total pressure of the system between 2 and 40 bars. At the wall, the temperature is obtained by iteration on the energy balance so that the heat flux through the condensed film equals the heat flux through the wall. The surrounding temperature of the external side of the wall is supposed to be constant and known. Eventually, the mass boundary condition at the wall is obtained by writing that, at steady state, the mass flux at the wall is equal to the flux of species consumed by the reaction of corrosion. The empirical correlation established by de Waard⁽³⁾ gives the reaction rate at the wall.

The effect of surface tension

At the very top of the pipe, condensed water will accumulate as droplets rather than form a film that would drain to the bottom of the pipe. In this case, the condensation rate is going to be lowered (in comparison to filmwise condensation) by the presence of these droplets, which minimize the contact surface with the bare metal and by the increase of the thermal resistance due to the thicker liquid phase. A material balance on the droplets leads to the equation:

$$\frac{dV}{dt} = \text{Cond.}R(t) \times S(t) \quad (7)$$

which leads to the growth rate of the droplet:

$$r(t) = \frac{3}{2} \left(-K + \sqrt{K^2 + \frac{4}{3} \times C \times t} \right) \quad (8)$$

where

$$C = \frac{\lambda \times (T_{\text{sat}} - T_{\text{ext}})}{\rho \times \Delta h_{\text{vap}}(T_{\text{sat}})} \quad \text{and} \quad K = \frac{2\lambda}{\lambda_{\text{wall}}} \times l$$

A droplet will remain attached to the pipe until the gravity forces overcome the forces due to the surface tension in the liquid phase. From a force balance applied to the droplet it is possible to determine the departure radius and the corresponding residence time of the droplet:

$$Rc = \sqrt{\frac{3 \times \sigma}{\rho \times g}} \quad (6)$$

$$t_{\text{dep}} = \frac{Rc^2 + 3 \times Rc \times K}{3 \times C} \quad (7)$$

Between the birth time of the droplet and its departure time, corrosion will take place, which tends to saturate the liquid droplet with corrosion products. The corrosion rate at the wall is still obtained from the de Waard correlation. In this case again, the wall temperature is obtained by iteration on the equation of the energy balance at the wall. The concentration of any species in the droplet is assumed to be homogeneous. The concentration of dissolved CO₂ is equal to the concentration in equilibrium with the gas phase according to Henry's law. The competition between the corrosion process and the condensation process determines the species concentrations. The two following formula give the concentrations of HCO₃⁻ and Fe²⁺ with respect to time:

$$[\text{Fe}^{2+}]_{t+\Delta t} = \frac{[\text{Fe}^{2+}]_t \times r^3(t)}{r^3(t+\Delta t)} + \frac{27 \times \Phi_{\text{Fe}}(t) \times \int_t^{t+\Delta t} (-K + \sqrt{K^2 + \frac{4}{3}Ct})^2 dt}{8 \times r^3(t+\Delta t)} \quad (8)$$

$$[\text{HCO}_3^-]_{t+\Delta t} = \frac{[\text{HCO}_3^-]_t \times r^3(t)}{r^3(t+\Delta t)} + \frac{27\Phi_{\text{Fe}}(t) \times \int_t^{t+\Delta t} (-K + \sqrt{K^2 + \frac{4}{3}Ct})^2 dt}{4 \times r^3(t+\Delta t)} \quad (9)$$

where $\Phi_{\text{Fe}}(t)$ is the corrosion rate expressed in mol/(m².s). The initial concentration of Fe²⁺ is zero and the initial concentration of HCO₃⁻ is given by solving the equation of dissolution and dissociation of carbon dioxide in absence of iron ions. The model is not dependent on the initial guess. Also the concentration profile with respect to time is calculated for the species H₂CO₃, CO₃²⁻, and H⁺. For each computational time step, the product [Fe²⁺] × [CO₃²⁻] is calculated and compared with the solubility product of iron carbonate. Thus, the saturation or supersaturation level is checked every time. Eventually the scaling tendency⁽⁶⁾ is calculated to check the possibility of the formation of a protective scale.

RESULTS AND DISCUSSION

Condensation rate in a horizontal pipe in presence of a non-condensable gas

According to the Equations 3 and 4, the condensation rate is a function of the saturation temperature and of the difference between the wall temperature and the outside temperature. The wall temperature is dependent on the film thickness according to Equation 3, which is dependent on the wall temperature and the saturation temperature according to Equation 1. It was chosen to present the estimated condensation rate as a function of the molar fraction of water in the gas phase for an outside temperature of 283K and a total pressure of 1bar. By doing so, we implicitly set all the other parameters that influence the condensation rate namely the saturation temperature, the film thickness, and the wall temperature. The pipe considered is a bare 4 inch stainless steel pipe with a heat transfer coefficient of 2.1 kW/m^2 . The results of the simulation can be seen in Figure 4, 5, and, 6. At low molar fraction of water in the gas phase, the changes in temperature at the wall are significant and therefore the condensation rate varies greatly. At higher molar fraction, the film thickness and the wall temperature don't vary very much and the condensation rate stabilizes.

Corrosion under filmwise condensation

The present Top Of the Line Corrosion model (TLC model) allows us to get a better estimation of the parameters that will influence the corrosion process, namely the wall temperature, the condensation rate, the dissolved carbon dioxide concentration at the wall, the pH, and the saturation level.

Influence of the condensate film on the wall temperature. Using Equations 2 and 3, the temperature profile at the wall was solved for the case of a bare stainless 4 inch pipe, schedule 40. The saturation temperature of the gas mixture was 321K and the surrounding temperature was 298K. The corresponding molar fraction of water in the gas phase was 11%. The results of simulation are shown in Figure 6. It is seen from the graph that the wall temperature stays within the range of 312K to 318K. Thus, the temperature at which the corrosion process takes place is up to 10K lower than the saturation temperature for this particular application. The corresponding condensation rate in this case is around $17 \text{ ml/m}^2/\text{s}$ according to Equation 4.

Influence of the condensate film on the concentration of corrosive species at the wall. The dissolved carbon dioxide concentration profile is obtained by solving the mass transport equation in the liquid film. As shown in Figure 7, it appears that the concentration at the wall is much lower than the concentration obtained in the thermodynamics equilibrium conditions (at the interface liquid-gas). The concentration at the wall progressively increases along the circumference of the pipe as the water flows downward.

Influence of the wall temperature and the concentration of CO₂ at the wall on the corrosion rate. In Figure 8, the corrosion rate calculated according to the TLC model is compared with the corrosion rate estimated by de Waard's⁽³⁾ correlation in non saturated conditions. It is seen that the TLC model gives much lower corrosion rates for the same bulk conditions. This is due to the influence of the condensate film as explained in the two previous paragraphs. Thus, the TLC model has the capacity to remove some

conservatism of the de Waard's correlation by carefully taking into consideration the local parameters at the wall instead of the bulk parameters.

Saturation of the liquid film. In order to determine if the saturation of the condensed water with Fe^{2+} is possible, the concentration profile in ferrous ions was computed (see Figure 9). As expected, the concentration of ferrous ion in the film can not build up and the ferrous iron is “washed away” even at distances of 10 μm from the wall by the condensing water. Thus, under filmwise condensation, the precipitation of an iron carbonate scale doesn't seem to be possible. This is confirmed by the case history presented by Gunaltun⁽⁴⁾ where it is described as the “washing effect”.

Influence of the surface tension. In the upper part of the pipe, the surface tension forces change the time that the condensed liquid remains in contact with the pipe. In this case, droplets form and grow at a rate determined by the condensation rate. The TLC model solves the chemistry of water with respect to time and takes into consideration the change in pH, saturation level, wall temperature, and the condensation rate to calculate the corrosion rate.

Computation of the condensation rate

As the droplet grows, the thermal resistance in the liquid phase increases and the wall temperature will become lower. The droplet grows in time according to the Equation 8. The corresponding condensation rate, which depends of the “thickness” of the droplet, is shown in Figure 10. The condensation rate tends to be much lower in the upper region compared to the side where the washing effect takes place. For the same bulk saturation temperature and pressure and for the same application as previously described, the condensation rate drops from 17 $\text{ml}/\text{m}^2/\text{s}$ (in the case of filmwise condensation) to 4 $\text{ml}/\text{m}^2/\text{s}$. This may be part of the explanation of the fact that the formation of a protective scale is possible in the upper region of the pipewall.

Computation of the corrosion rate

According to the significant amount of time needed before a droplet reaches its critical size and falls from the wall, the assumption is made that the diffusion of species is not a limiting factor. Therefore the concentrations of species are homogeneous in the droplet. The corrosion rate is calculated taking into account that the temperature at the wall decreases with time. Using the kinetics of reaction suggested by de Waard, it appears that the droplet becomes saturated no matter what the condensation rate is (the higher condensation rate simulated was 25 $\text{ml}/\text{m}^2/\text{s}$ and in this case as well, saturation would be reached). Another way to predict the kinetics of corrosion reaction is needed in the case of saturated or supersaturated bulk.

CONCLUSIONS

The prediction of the corrosion rate for Top-Of-The-Line Corrosion requires an accurate estimation of the condensation rate. A model was proposed that predicts the condensation rate in both situations where water condenses as a film that drains to the bottom of the pipe or as droplets that remain stagnant at the top of the pipe before falling under the influence of gravity forces. Preliminary results show that under filmwise condensation no saturation of the liquid film is possible. In such a case, the model, by considering the temperature and concentration of carbon dioxide at the wall rather than in

the bulk, predicts less conservative results when using deWaard's correlation. In the case where condensation rates are obtained by taking into consideration the accumulation of water as droplets deWaard's correlation leads to saturation conditions, no matter which condensation rate is considered.

REFERENCES

1. M. Estavoyer, "Corrosion problems at Lack sour gas field", NACE publication "H₂S corrosion in oil and gas production", page 905, Houston Texas, 1981.
2. S. Olsen, A. Dugstad, "Corrosion under Dewing conditions", Corrosion /91, paper no. 472, (Houston, TX: NACE International 1991).
3. C. de Waard, U. Lotz, "Prediction of CO₂ corrosion of carbon steel", Corrosion/93, paper no. 69, (Houston, TX: NACE International, 1993).
4. Y M Gunaltun, D Supriyataman, A Jumaludin, "Top of the line corrosion in multiphase gas lines. A case history", Corrosion/99, paper no. 36, (Houston, TX: NACE International 1999).
5. B. F. M. Pots , E. L. J. A Hendriksen, "CO₂ corrosion under scaling conditions - the special case of top-of-line corrosion in wet gas pipelines", Corrosion 2000, paper no 31, (Houston, TX: NACE International 2000).
6. E. W. J. Van Hunnik, "The formation of protective FeCO₃ corrosion product layers in CO₂ corrosion, Corrosion/96, paper no 6, (Houston, TX: NACE International 1996).
7. J.E Oddo, M.B Tomson, "Simplified Calculation of CaCO₃ Saturation at High Temperatures and pressures in Brine Solutions". SPE of AIME, (1982): p 1583.
8. Y.M Gunaltun, D Larrey: "Correlation of cases of Top of the line Corrosion with calculated condensation rates", Corrosion/2000, paper no. 71, (Houston, TX: NACE International 2000).
9. M. A Edwards, B. Cramer, "Top of the Line Corrosion – Diagnosis, Root Cause Analysis, and treatment", Corrosion/2000, paper no. 72, Houston, TX: NACE International 2000).
10. G. Schmitt, M. Scheepers, G. Siegmund, "Inhibition of the Top of the line Corrosion under stratified flow", Corrosion/2001, paper no. 1032, (Houston, TX: NACE International 2001).
11. Y. M. Gunaltun, A. Belghazi, "Control of the Top of the line corrosion by chemical treatment": Corrosion 2001, paper no. 33, Houston, TX: NACE International 2001)..
12. W. Nusselt, Die Oberflächenkondensation des Wasserdampfes. VDI Z. 60(1916), p 441, p569.
13. A. Fenghour, W. A. Wakenham, J.T.R Watson, J. Chem. Thermodynamics 28, (1996): p 433.

LIST OF SYMBOLS

Symbol	Name	SI-Units
A, A'	constants	-
B, B'	constants	-
C, C'	constants	-
Cond. R	condensation rate	$\text{m}^3/\text{m}^2/\text{s}$
g	gravitational constant	m/s^2
$h(\varphi)$	heat transfer coefficient averaged over the angle φ	$\text{W}/\text{m}^2/\text{K}$
l	thickness of pipe	m
\dot{m}	condensation rate	$\text{kg}/\text{m}^2/\text{s}$
P_w^{sat}	saturation pressure of the vapor	Pa
P	total pressure	Pa
r	Radius of a droplet	m
R	Radius of the pipe	m
R_c	Critical radius of a droplet	m
S	surface of the base of a droplet	m^3/s
T_{ext}	outside temperature	K
T_{sat}	temperature at saturation	K
T_{wall}	temperature at the wall	K
V	volume of a droplet	m^3/s
x_w	mole fraction of water in the liquid phase	-
y_w	mole fraction of water in the vapor phase	-
δ	thickness of the momentum boundary layer in the liquid	m
Δh_v	specific enthalpy of vaporization	J/kg
ε	void fraction	-
φ	circumferential angle	-
λ_l	thermal conductivity of the liquid phase	$\text{W}/\text{K}/\text{m}$
λ_{wall}	thermal conductivity of the wall	$\text{W}/\text{K}/\text{m}$
μ_l	dynamic gas viscosity in the liquid phase	$\text{kg}/\text{s}/\text{m}$
μ_g	dynamic viscosity in the gas phase	$\text{kg}/\text{s}/\text{m}$
ρ_g	density of the gas phase	kg/m^3
ρ_l	liquid density	kg/m^3

TABLE 1
CONDENSATION RATE AS A FUNCTION OF THE MASS FRACTION OF WATER IN
THE GAS PHASE

Total Pressure: 1 bar		Outside temperature: 283 K	
Mass fraction	Wall temperature (K)	Thickness (μm)	Condensation rate (ml/m ² .s)
0.005	283.3	25	0.22
0.006	285.6	45	2.1
0.007	287.5	53	3.8
0.008	289.1	57.3	5.62
0.009	290.6	60.9	6.98
0.01	291.5	63	8.2
0.02	301	71	15.8
0.03	304.3	74.2	21
0.04	310.6	76	24.8
0.05	313.8	77.1	27.8
0.1	323.9	79.8	37.6
0.5	345	83.9	60.8
1	353.3	84.6	68

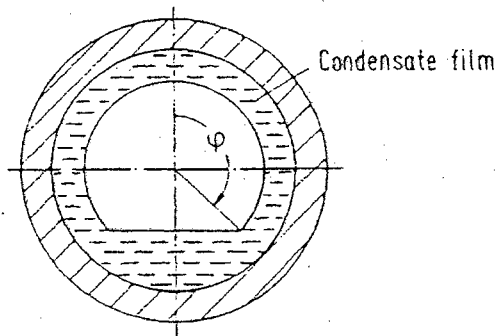


FIGURE 1- Cross section of a pipe during condensation under stratified flow conditions

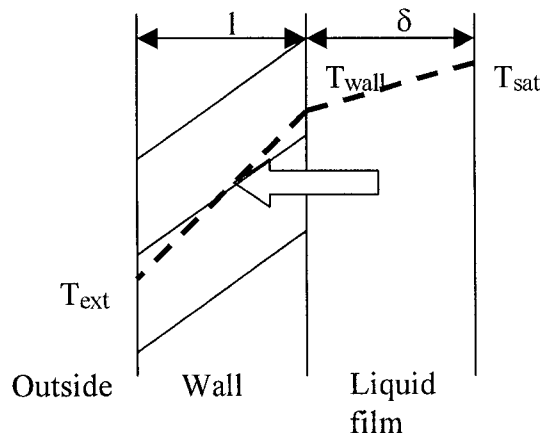


FIGURE 2 – Heat flux at the wall

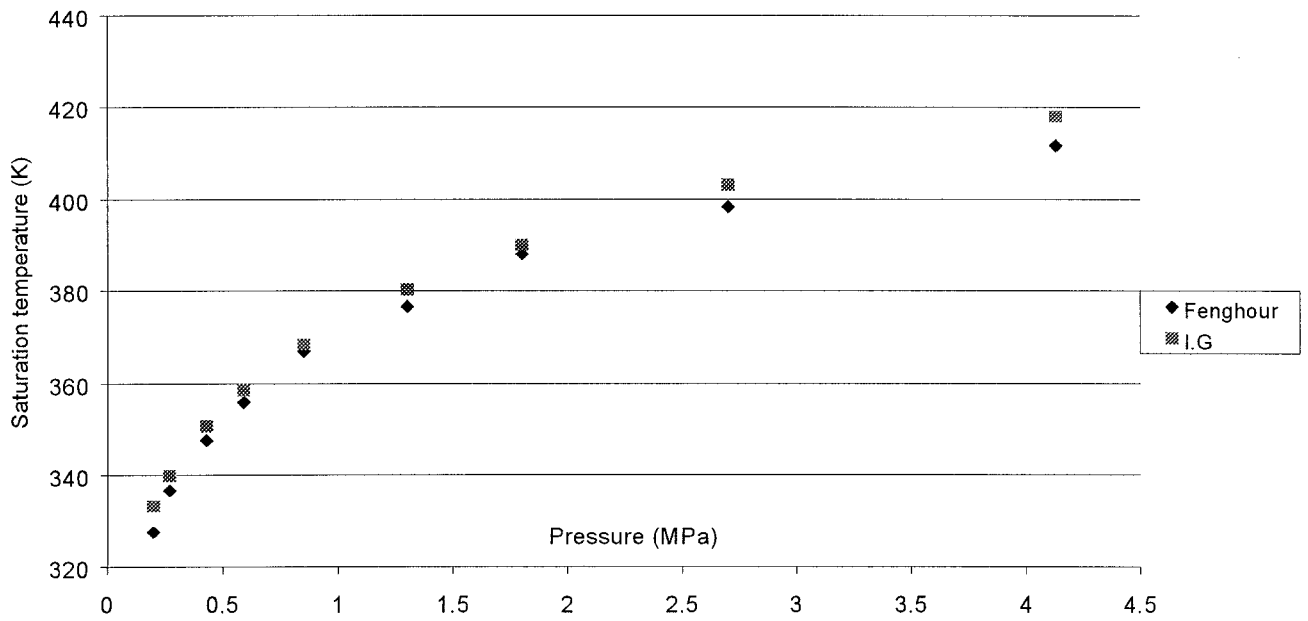


FIGURE 3 – Comparison between the experimental data from Fenghour and the ideal gas law for the saturation temperature of water in CO₂-H₂O mixture, $y_{H_2O}=0.1$

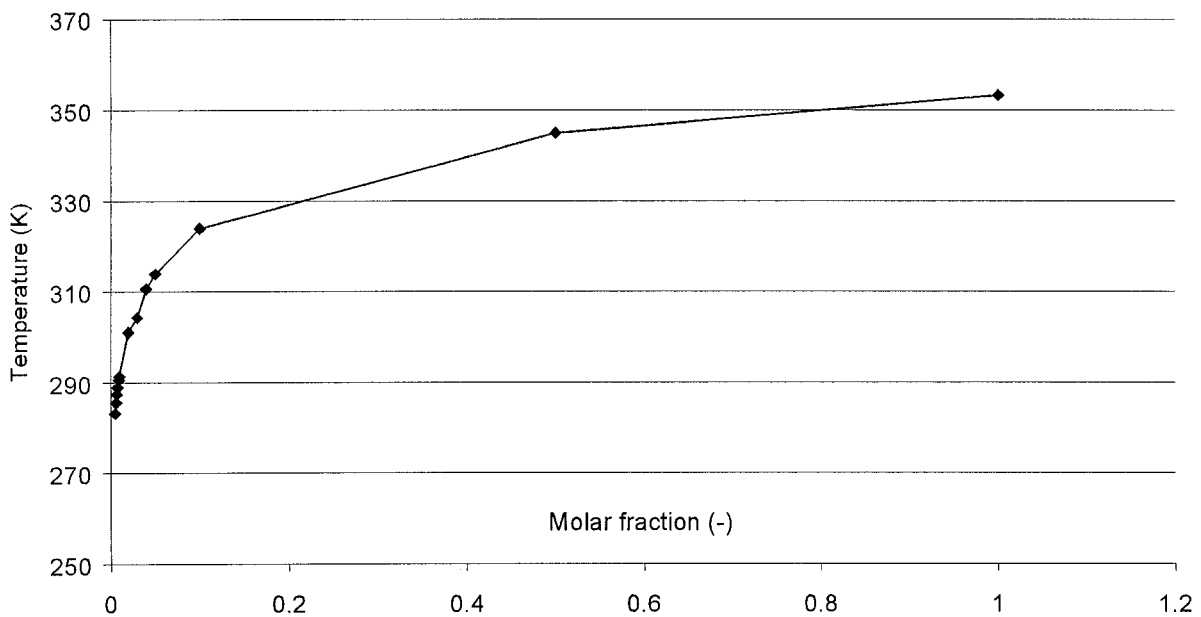


FIGURE 4 – Wall temperature as a function of the molar fraction of water in the gas phase ($P=1$ bar, $T_{ext} = 283$ K)

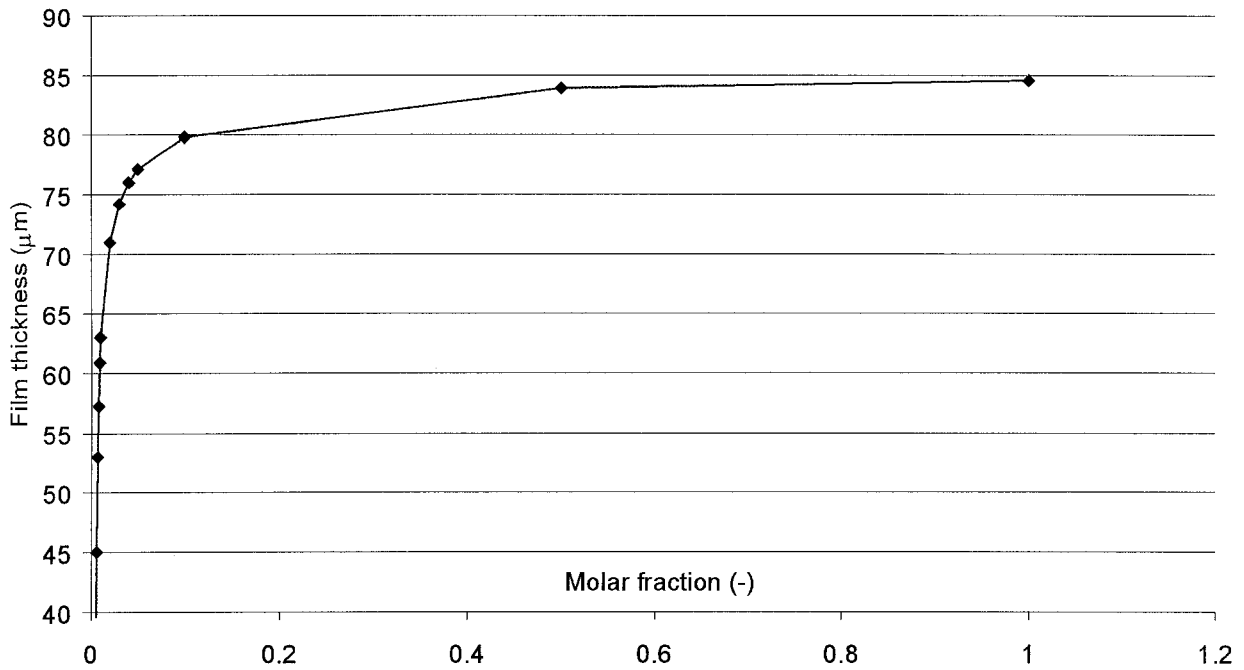


FIGURE 5 – Average film thickness as a function of the molar fraction of water in the gas phase (P= 1bar, Text= 283K)

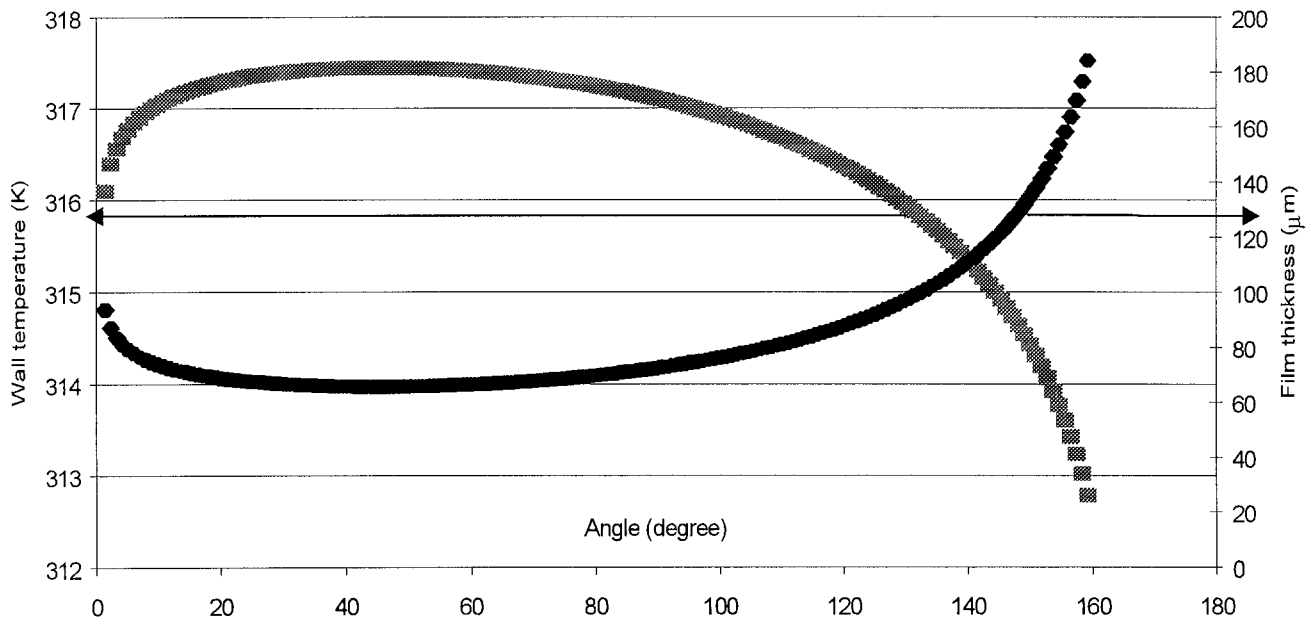


FIGURE 6 – Wall temperature and film thickness profile along the inner wall of the cross section of an horizontal pipe. Tsat= 320K, Text= 298K, Radius = 0.055m, h = 2.1kw/m².K

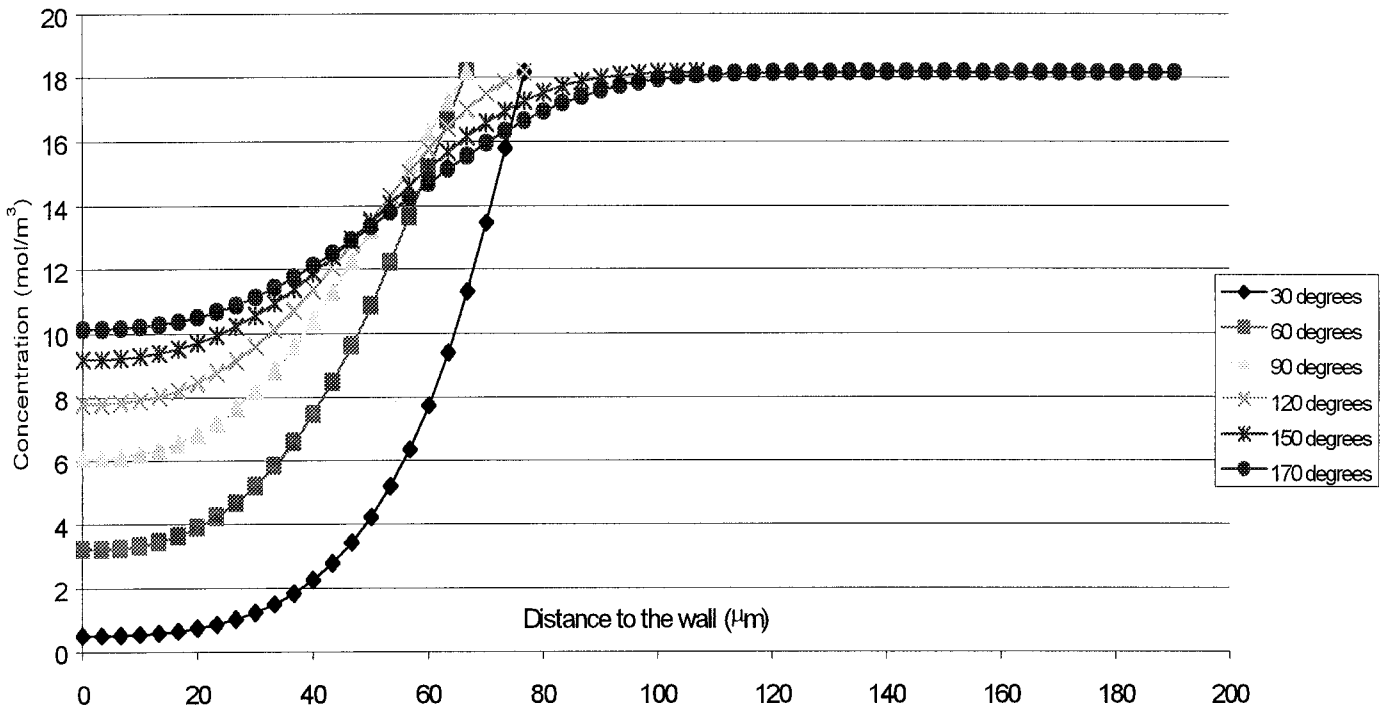


FIGURE 7 – Dissolved CO₂ concentration profile in the condensed film at different positions around the circumference of the pipe

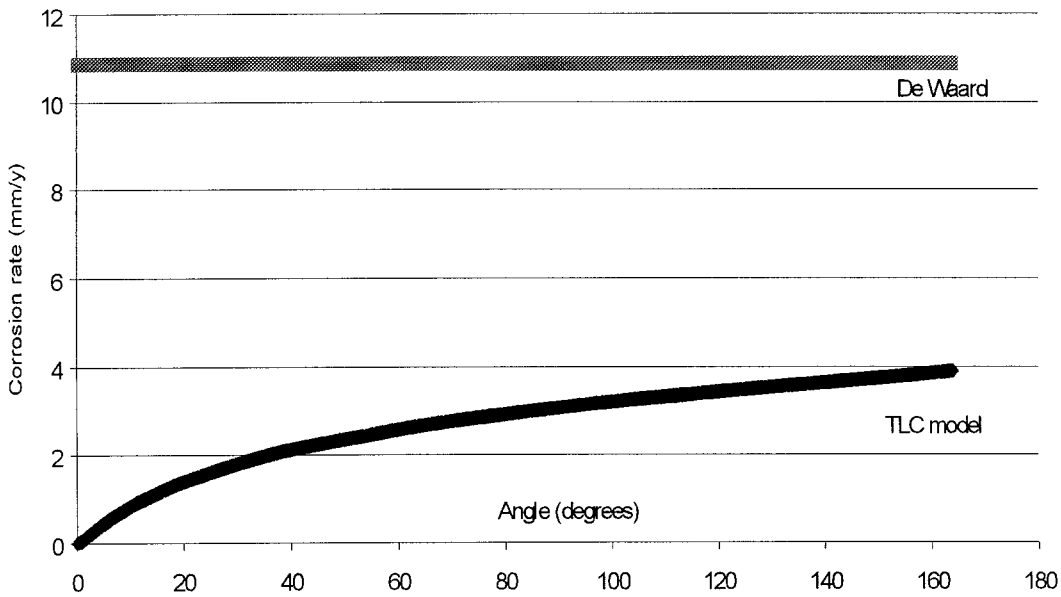


FIGURE 8 – Corrosion rate as a function of the circumferential angle. $T_{sat} = 321K$, $T_{ext} = 298 K$, $P_{tot} = 1.1 \text{ bar}$, $P_{CO_2} = 1 \text{ bar}$, $x_{H_2O} = 0.11$

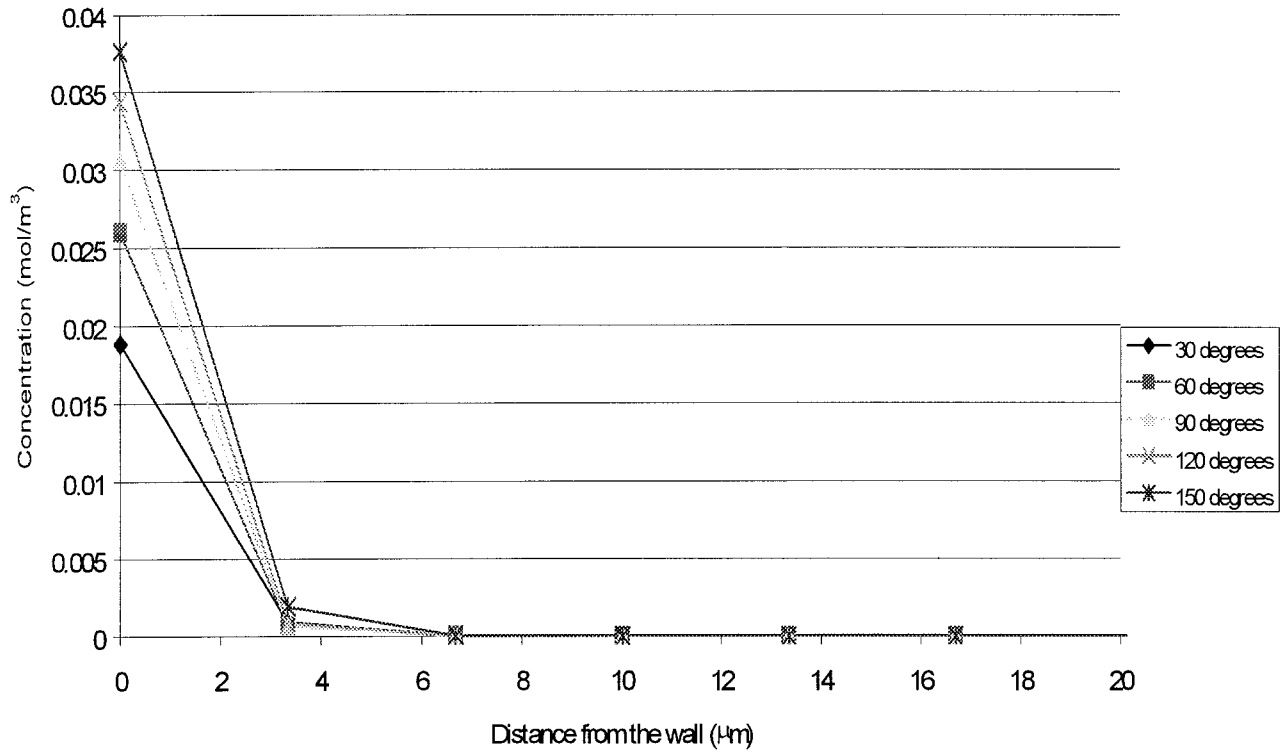


FIGURE 9 – Concentration profile of iron ions in the condensed film at different positions around the circumference of the pipe

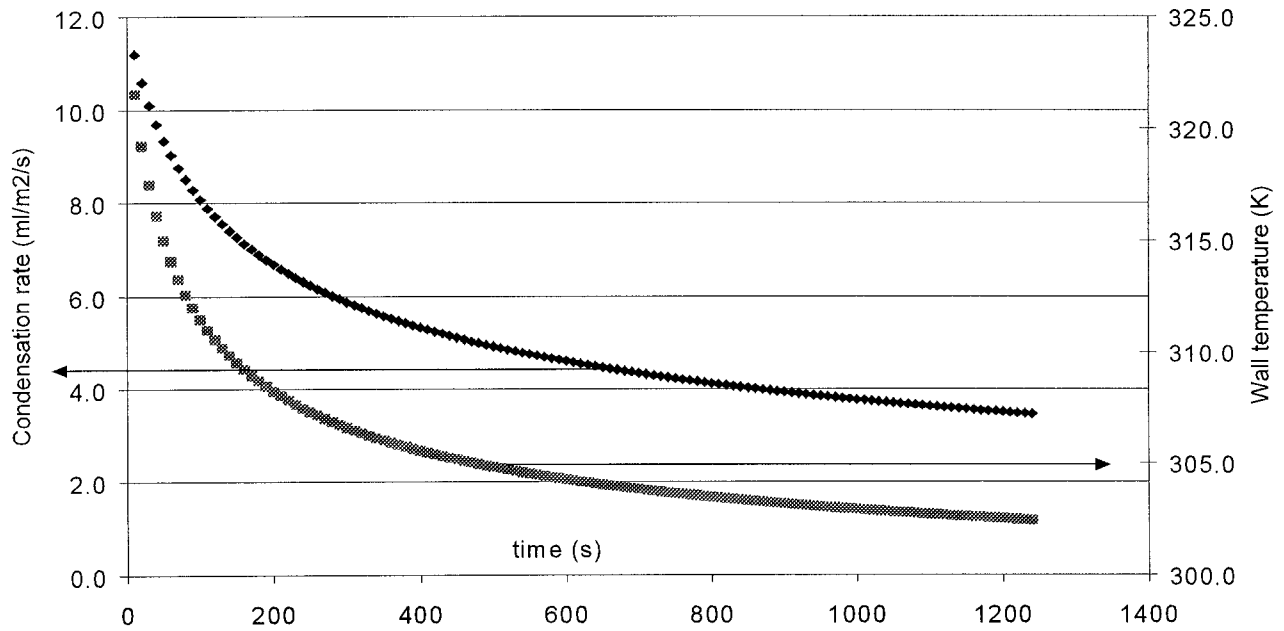


FIGURE 10 – Condensation rate and wall temperature as a function of time. $T_{sat} = 323K$, $T_{ext} = 298K$, $x_{H_2O} = 0.11$, $P_{tot} = 1.1 \text{ bar}$, $h = 2.1 \text{ kW/m}^2 \cdot K$